Arch Appl Mech (2007) 77: 197–214
DOI 10.1007/s00419-006-0084-y

ORIGINAL

A. M. Zenkour

Benchmark trigonometric and 3-D elasticity solutions for an exponentially graded thick rectangular plate

Received: 27 December 2005 / Accepted: 6 September 2006 / Published online: 24 October 2006

Abstract The bending problem of a transverse load acting on an isotropic inhomogeneous rectangular plate using both two-dimensional (2-D) trigonometric and three-dimensional (3-D) elasticity solutions is considered. In the present 2-D solution, trigonometric terms are used for the displacements in addition to the initial terms of a power series through the thickness. The effects due to transverse shear and normal deformations are both included. The form of the assumed 2-D displacements is simplified by enforcing traction-free boundary conditions at the faces of the plate. No transverse shear correction factors are needed because a correct representation of the transverse shearing strain is given. The plate material is exponentially graded, meaning that Lamé's coefficients vary exponentially in a given fixed direction (the thickness direction). A wide variety of results for the displacements and stresses of an exponentially graded rectangular plate are presented. The validity of the present 2-D trigonometric solution is demonstrated by comparison with the 3-D elasticity solution. The influence of aspect ratio, side-to-thickness ratio and the exponentially graded parameter on the bending response are investigated.

Keywords Trigonometric shear deformation theory · 3-D elasticity solution · Exponentially grading · Thick plate

1 Introduction

In recent years, functionally graded materials (FGMs) have received considerable attention in many engineering applications. FGMs are an alternative to homogeneous, microscopically inhomogeneous, in which the mechanical properties vary smoothly and continuously from one surface to the other. Several studies have been performed to analyse the behaviour of FGM plates and shells [1–10]. Analytical three-dimensional (3-D) solutions for FGM plates are useful since they provide benchmark results to assess the accuracy of various 2-D plate theories and finite-element formulations (see, e.g., [8–10]).

Based on the two-dimensional (2-D) plate theory, many investigations concerning problems of inhomogeneous plates have been published in (see, e.g., [11–18]). For thin plates, almost all of the analyses were based on classical assumptions, such as the Love–Kirchhoff hypothesis that ignored transverse shear deformations and thickness changes. The classical theory predicts the response of thin plates with reasonable accuracy, yet it usually fails to yield similar accuracy for thick plates or composite plates of a similar configuration; it

A. M. Zenkour (✉)
Department of Mathematics, Faculty of Education, Kafr El-Sheikh University, Kafr El-Sheikh 33516, Egypt
E-mail: zenkour@hotmail.com

Present address: Department of Mathematics, Faculty of Science, King AbdulAziz University, P.O. Box 80203, Jeddah 21589, Saudi Arabia
E-mail: zenkour@kau.edu.sa

underestimates deflection and overestimates natural frequencies and buckling loads. In addition, it is plagued with inconsistency between the order of the governing equation and the number of boundary conditions.

Many plate theories that account for transverse shear deformations exist. In Reissner–Mindlin-based theories, the displacement field accounts for linear or higher-order variations of mid-plane displacements through the thickness [19–26]. In higher-order theories, an additional dependent unknown is introduced into the theory with each additional power of the thickness coordinate. In addition, these shear deformation theories do not satisfy the conditions of zero transverse shear stresses on the top and bottom surfaces of the plate, and require a shear correction to the transverse shear stiffnesses. The first-order shear deformation plate theory (FPT) assumes that the in-plane displacement field is linear and the transverse deflection is constant through the thickness. FPT results in a fairly accurate global response for isotropic materials when used with an appropriate shear correction factor, even though a parabolic transverse shear-strain distribution through the thickness is not described. Many theories have been developed to overcome this deficiency of FPT. Some of these theories account not only for transverse shear strains, but also for a parabolic variation of the transverse shear stresses through the thickness, and consequently there is no need to use shear correction coefficients in computing the shear stresses (see, e.g., [3–6,16–18,20–30]).

Rather than looking for general techniques, we concentrate here on a specific inhomogeneous material, one that has found application in functionally graded materials. Thus, we assume that the material properties vary in a simple, explicit manner. Here, we consider exponential variations, and suppose that the plate is isotropic with variable Lamé's coefficients. The trigonometric shear deformation plate theory (TPT) presented by Zenkour [25–30] is modified for the bending response of an exponentially graded material plate. This theory is simplified by enforcing traction-free boundary conditions at the faces of the plate. The effects of shear and normal deformation are both included. To assure the accuracy of the present theory, the convergence of the displacements and stresses are compared with those obtained using the 3-D elasticity solution. The trigonometric and 3-D elasticity solutions are important because they can be used to study the behaviour of EGM thick rectangular plates, in addition to serving as references for future approximate solutions by numerical methods and other 2-D plate theories.

2 Bending analysis according to a trigonometric shear deformation theory

2.1 Formulation of the problem

Consider an undeformed rectangular $(a \times b)$ plate of uniform thickness h made of an isotropic material. We use a rectangular Cartesian coordinate system $\{x_i\}$ $(i = 1, 2, 3)$, with the plane $x_3 = 0$ coincident with the mid-surface of the plate. A normal traction $\sigma_{33} = q(x_1, x_2)$ is applied on the upper surface, while the lower surface is traction free (Fig. 1). Here, the material is inhomogeneous and functionally graded; specifically, the plate is exponentially graded (EG). We assume that the composition varies from the bottom to the top surfaces according to a simple exponential law. In such a way, the effective material properties P, like Lamé's coefficients, can be expressed as

$$P = P_0 f(x_3), \quad f(x_3) = e^{k(x_3/h+1/2)}, \quad k \neq 0, \tag{2.1}$$

where $P_b = P_0$ and $P_t = P_0 e^k$ denote the properties of the bottom and top surfaces of the plate, respectively, and P_0 is the material properties of the homogeneous plate. Note that k is a parameter that dictates the material variation profile through the plate thickness and takes values greater than zero. In the case $k = 0$, the plate is fully homogeneous.

The trigonometric plate theory (TPT) presented here is appropriate to the following displacement forms:

$$\left.\begin{aligned} v_\alpha(x_i) &= u_\alpha - x_3 u_{3,\alpha} + \Psi \varphi_\alpha, \\ v_3(x_i) &= u_3 + \Psi_{,3} \varphi_3, \end{aligned}\right\} \tag{2.2}$$

where u_i and φ_i depend upon the in-plane coordinates x_α and

$$\Psi(x_3) = \frac{h}{\pi} \sin\left(\frac{\pi x_3}{h}\right). \tag{2.3}$$

Note that a comma followed by index j, for example, denotes partial differentiation with respect to the position x_j of a material particle, with Latin indices ranging from 1 to 3 and Greek indices from 1 to 2. Hereafter, a repeated index implies summation over the range of the index.

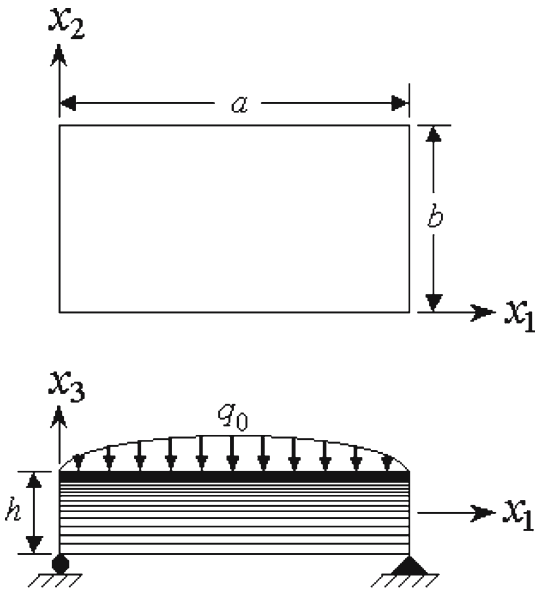

Fig. 1 The EGM plate geometry and coordinate system

The present theory is simplified by enforcing traction-free boundary conditions at the top and bottom surfaces of the plate. The effects of shear and normal deformation are both included. This theory contains only one of the additional dependent unknowns of first- and third-order shear deformation theories, but takes accounts of the transverse shear strains through the thickness of the plate using a cosine-law distribution. No transverse shear correction factors are needed for the TPT because a correct representation of the transverse shearing strain is given.

For the displacement field in Eq. (2.2), the linear strains $e_{ij} = \frac{1}{2}(v_{i,j} + v_{j,i})$ are:

$$\begin{aligned} e_{\alpha\beta} &= \varepsilon_{\alpha\beta} + x_3\kappa_{\alpha\beta} + \Psi\eta_{\alpha\beta}, \\ e_{\alpha 3} &= \Psi_{,3}\varepsilon_{\alpha 3}, \\ e_{33} &= \Psi_{,33}\varepsilon_{33}. \end{aligned} \tag{2.4}$$

Here the non-vanishing strain measures $e_{ij} \equiv e_{ij}(x_\omega)$ are expressed in terms of the displacement quantities as:

$$\begin{aligned} \varepsilon_{\alpha\beta} &= \tfrac{1}{2}(u_{\alpha,\beta} + u_{\beta,\alpha}), \\ \eta_{\alpha\beta} &= \tfrac{1}{2}(\varphi_{\alpha,\beta} + \varphi_{\beta,\alpha}), \\ \kappa_{\alpha\beta} &= -u_{3,\alpha\beta}, \\ \varepsilon_{\alpha 3} &= \tfrac{1}{2}(\varphi_\alpha + \varphi_{3,\alpha}), \\ \varepsilon_{33} &= \varphi_3. \end{aligned} \tag{2.5}$$

The stress–strain relations for a linear isotropic elastic plate are given by

$$\sigma_{ij} = \lambda\theta\delta_{ij} + 2\mu e_{ij}, \tag{2.6}$$

where λ and μ are the Lamé's coefficients, $\theta = e_{11} + e_{22} + e_{33}$, and δ_{ij} is the Kronecker's delta. Here we assume that the material properties λ and μ vary according to Eq. (2.1),

$$\lambda = \lambda_0 f(x_3), \quad \mu = \mu_0 f(x_3), \tag{2.7}$$

in which

$$\lambda_0 = \frac{\nu E_0}{(1+\nu)(1-2\nu)}, \quad \mu_0 = \frac{E_0}{2(1+\nu)}, \tag{2.8}$$

where E_0 and ν are the Young's modulus and Poisson's ratio, respectively, and $f(x_3)$ represents the exponential variations of Lamé's coefficients in the thickness direction. So, we say that the plate is exponentially graded in terms of the parameter k. Evidently Poisson's ratio is constant for such a plate.

We introduce the following definitions of the stress resultants:

$$(N_{\alpha\beta}, M_{\alpha\beta}, P_{\alpha\beta}) = \int_{-h/2}^{h/2} (1, x_3, \Psi)\sigma_{\alpha\beta}\mathrm{d}x_3, \tag{2.9a}$$

$$Q_{\alpha 3} = \int_{-h/2}^{h/2} \Psi_{,3}\sigma_{\alpha 3}\mathrm{d}x_3, \tag{2.9b}$$

$$N_{33} = \int_{-h/2}^{h/2} \Psi_{,33}\sigma_{33}\mathrm{d}x_3, \tag{2.9c}$$

where $N_{\alpha\beta}$ and $M_{\alpha\beta}$ are the basic components of the stress resultants and stress couples; $P_{\alpha\beta}$ are additional stress couples associated with the transverse shear effects, and $Q_{\alpha 3}$ and N_{33} are transverse and normal shear stress resultants.

2.2 Governing equations

The governing equations of the equilibrium associated with the displacement field in Eq. (2.2) are:

$$\begin{aligned} N_{\alpha\beta,\beta} &= 0, \\ M_{\alpha\beta,\alpha\beta} &= 0, \\ P_{\alpha\beta,\beta} - Q_{\alpha 3} + q &= 0, \\ Q_{\alpha 3,\alpha} - N_{33} &= 0. \end{aligned} \tag{2.10}$$

Using Eq. (2.6) in Eq. (2.9), the stress resultants can be related to the total strains by

$$\begin{Bmatrix} N_{\alpha\beta} \\ M_{\alpha\beta} \\ P_{\alpha\beta} \end{Bmatrix} = [A]\begin{Bmatrix} \varepsilon_{\alpha\beta} \\ \kappa_{\alpha\beta} \\ \eta_{\alpha\beta} \end{Bmatrix} + \left([B]\begin{Bmatrix} \varepsilon_{11}+\varepsilon_{22} \\ \kappa_{11}+\kappa_{22} \\ \eta_{11}+\eta_{22} \end{Bmatrix} + [C]\varepsilon_{33} \right)\delta_{\alpha\beta}, \tag{2.11a}$$

$$N_{33} = c\varepsilon_{33} + [C]^T \begin{Bmatrix} \varepsilon_{11}+\varepsilon_{22} \\ \kappa_{11}+\kappa_{22} \\ \eta_{11}+\eta_{22} \end{Bmatrix}, \quad Q_{\alpha 3} = 2c^*\varepsilon_{\alpha 3}, \tag{2.11b}$$

where

$$\begin{aligned} [A] &= \int_{-h/2}^{h/2} 2\mu[F]\mathrm{d}x_3, \quad [B] = \int_{-h/2}^{h/2} \lambda[F]\mathrm{d}x_3, \\ [C] &= \int_{-h/2}^{h/2} \lambda\Psi_{,33}\begin{bmatrix} 1 \\ x_3 \\ \Psi \end{bmatrix}\mathrm{d}x_3, \quad c = \int_{-h/2}^{h/2} (2\mu+\lambda)(\Psi_{,33})^2\mathrm{d}x_3, \quad c^* = \int_{-h/2}^{h/2} \mu(\Psi_{,3})^2\mathrm{d}x_3, \end{aligned} \tag{2.12}$$

in which

$$[F] = \begin{bmatrix} 1 & x_3 & \Psi \\ x_3 & x_3^2 & x_3\Psi \\ \Psi & x_3\Psi & \Psi^2 \end{bmatrix}. \tag{2.13}$$

Substitution from Eq. (2.11) into Eq. (2.10) results in the following field equations in terms of the six displacement functions u_i and φ_i:

$$\begin{aligned}
&\left(A^{11}+B^{11}\right)u_{1,11}+\tfrac{1}{2}A^{11}u_{1,22}+\left(\tfrac{1}{2}A^{11}+B^{11}\right)u_{2,12}-\left(A^{12}+B^{12}\right)\nabla^2 u_{3,1}\\
&\quad+\left(A^{13}+B^{13}\right)\varphi_{1,11}+\tfrac{1}{2}A^{13}\varphi_{1,22}+\left(\tfrac{1}{2}A^{13}+B^{13}\right)\varphi_{2,12}\\
&\quad+C^{11}\varphi_{3,1}=0\quad(1\leftrightarrow 2)\,, \qquad (2.14a)\\
&\left(A^{12}+B^{13}\right)\left(\nabla^2 u_{1,1}+\nabla^2 u_{2,2}\right)-\left(A^{22}+B^{22}\right)\nabla^4 u_3+\left(A^{23}+B^{23}\right)\left(\nabla^2\varphi_{1,1}\right.\\
&\quad\left.+\nabla^2\varphi_{2,2}\right)+C^{12}\nabla^2\varphi_3+q=0, \qquad (2.14b)\\
&\left(A^{13}+B^{13}\right)u_{1,11}+\tfrac{1}{2}A^{13}u_{1,22}+\left(\tfrac{1}{2}A^{13}+B^{13}\right)u_{2,12}-\left(A^{23}+B^{23}\right)\nabla^2 u_{3,1}\\
&\quad+\left(A^{33}+B^{33}\right)\varphi_{1,11}+\tfrac{1}{2}A^{33}\varphi_{1,22}+\left(\tfrac{1}{2}A^{33}+B^{33}\right)\varphi_{2,12}-c^*\varphi_1\\
&\quad+\left(C^{13}-c^*\right)\varphi_{3,1}=0\quad(1\leftrightarrow 2)\,, \qquad (2.14c)\\
&C^{11}\left(u_{1,1}+u_{2,2}\right)-C^{12}\left(u_{3,11}+u_{3,22}\right)+\left(C^{13}-c^*\right)\left(\varphi_{1,1}+\varphi_{2,2}\right)+c\varphi_3\\
&\quad-c^*\left(\varphi_{3,11}+\varphi_{3,22}\right)=0, \qquad (2.14d)
\end{aligned}$$

where A^{ij} and B^{ij} are the elements of the symmetric matrices $[A]$ and $[B]$, respectively. Also, the sign $(1\leftrightarrow 2)$ indicates that other equations may be obtained from Eqs. (2.14a) and (2.14c) by changing the subindex from 1 to 2 and vice versa. $\nabla^2(\,)=(\,)_{,11}+(\,)_{,22}$ is the two-dimensional *Laplace* operator. Note that A^{12}, A^{13}, B^{12}, B^{13} and C^{11} vanish for a plate that is materially and geometrically symmetric about its mid-surface.

2.3 Two-dimensional solution

Rectangular plates are generally classified according to the type of support used. Here, we are concerned with the exact solutions of Eqs. (2.14) for a simply supported EGM plate. The following boundary conditions are imposed at the side edges:

$$\begin{aligned}
&N_{11}=M_{11}=S_{11}=u_2=u_3=\varphi_2=\varphi_3=0\quad\text{at } x_1=0,a,\\
&N_{22}=M_{22}=S_{22}=u_1=u_3=\varphi_1=\varphi_3=0\quad\text{at } x_2=0,b. \qquad (2.15)
\end{aligned}$$

To solve this problem, Navier presented the external force in the form of a double trigonometric series

$$q(x_1,x_2)=\sum_{m=1}^{\infty}\sum_{n=1}^{\infty}q_{mn}\sin(\alpha_m x_1)\sin(\beta_n x_2), \qquad (2.16)$$

where $\alpha_m=m\pi/a$, $\beta_n=n\pi/b$, and m and n are mode numbers. For the case of a sinusoidally distributed load, we have

$$m=n=1\quad\text{and}\quad q_{11}=q_0, \qquad (2.17)$$

where q_0 represents the intensity of the load at the plate centre.

Following the Navier solution procedure, we assume the following solution form for u_i and φ_i that satisfies the boundary conditions given in Eq. (2.15),

$$\begin{Bmatrix} u_1\\ u_2\\ u_3\\ \varphi_1\\ \varphi_2\\ \varphi_3 \end{Bmatrix}=\sum_{m=1}^{\infty}\sum_{n=1}^{\infty}\begin{Bmatrix} U_1^{mn}\cos(\alpha_m x_1)\sin(\beta_n x_2)\\ U_2^{mn}\sin(\alpha_m x_1)\cos(\beta_n x_2)\\ U_3^{mn}\sin(\alpha_m x_1)\sin(\beta_n x_2)\\ \Phi_1^{mn}\cos(\alpha_m x_1)\sin(\beta_n x_2)\\ \Phi_2^{mn}\sin(\alpha_m x_1)\cos(\beta_n x_2)\\ \Phi_3^{mn}\sin(\alpha_m x_1)\sin(\beta_n x_2) \end{Bmatrix}. \qquad (2.18)$$

Here U_1^{mn}, U_2^{mn}, U_3^{mn}, Φ_1^{mn}, Φ_2^{mn} and Φ_3^{mn} are arbitrary parameters. Equations (2.14) in conjunction with Eq. (2.18) can be combined into a system of first-order equations:

$$[L]\{\Delta\}=\{f\}, \qquad (2.19)$$

where $\{\Delta\}$ and $\{f\}$ denote the columns

$$\{\Delta\}^{\mathrm{T}} = \left\{U_1^{mn}, U_2^{mn}, U_3^{mn}, \Phi_1^{mn}, \Phi_2^{mn}, \Phi_3^{mn}\right\}$$
$$\{f\}^{\mathrm{T}} = \{0, 0, -q_{mn}, 0, 0, 0\}, \tag{2.20}$$

where the superscript T denotes the transpose of the given vector. The elements $L_{ij} = L_{ji}$ of the coefficient matrix $[L]$ are defined in Appendix A. Thus, one can easily solve the 6×6 matrix equation (2.19) for the vector of amplitudes of the arbitrary parameters U_1^{mn}, U_2^{mn}, U_3^{mn}, Φ_1^{mn}, Φ_2^{mn} and Φ_3^{mn}. From these parameters, the corresponding displacements u_i and φ_i and the stresses σ_{ij} can be obtained.

3 Three-dimensional elasticity solution

In this section we present a more general procedure for solving the exact 3-D elasticity equations and generate extensive numerical results for EGM plates [31]. The exact results will be compared with those obtained by the trigonometric shear deformation plate theory (TPT). This way, a more accurate assessment can be obtained concerning the validity of the 2-D plate theory for EGM plates.

We let $v_i(x_1, x_2, x_3)$ denote the displacement components of a material point located at (x_1, x_2, x_3) of the EGM plate in the x_1, x_2, and x_3 directions, respectively. The equations of equilibrium in the absence of body forces are

$$\sigma_{ij,j} = 0 \quad (i, j = 1, 2, 3), \tag{3.1}$$

where σ_{ij} are components of the Cauchy stress tensor defined in Eq. (2.6). Substitution of Eq. (2.6) into the equations of equilibrium leads to

$$\mu\nabla^2 v_i + (\lambda + \mu)\theta_{,3} + \mu_{,3}(v_{i,3} + v_{3,i}) + \lambda_{,3}\theta\delta_{i3} = 0, \tag{3.2}$$

where $\nabla^2(\,) = (\,)_{,11} + (\,)_{,22} + (\,)_{,33}$.

Since the EGM plate is simply supported on the sides $x_1 = 0, a$ and $x_2 = 0, b$, the boundary conditions on these sides are prescribed by the normal traction and the tangential displacements being equal to zero, so that:

$$\begin{aligned} &\sigma_{11} = v_2 = v_3 = 0 \quad \text{at } x_1 = 0, a, \\ &\sigma_{22} = v_1 = v_3 = 0 \quad \text{at } x_2 = 0, b. \end{aligned} \tag{3.3}$$

These conditions are satisfied by assuming

$$\begin{Bmatrix} v_1 \\ v_2 \\ v_3 \end{Bmatrix} = \sum_{m=1}^{\infty}\sum_{n=1}^{\infty} \begin{Bmatrix} V_1^{mn}(x_3)\ \cos(\alpha_m x_1)\ \sin(\beta_n x_2) \\ V_2^{mn}(x_3)\ \sin(\alpha_m x_1)\ \cos(\beta_n x_2) \\ V_3^{mn}(x_3)\ \sin(\alpha_m x_1)\ \sin(\beta_n x_2) \end{Bmatrix}. \tag{3.4}$$

Substitution of Eq. (3.4) into Eq. (3.2) yields a system of second-order ordinary differential equations in the x_3-coordinate. After some elementary manipulations, the obtained set of equations takes the form:

$$\begin{aligned} V_{1,33}^{mn} &= c_1 V_1^{mn} + c_2 V_2^{mn} + c_3 V_3^{mn} + c_4 V_{1,3}^{mn} + c_5 V_{3,3}^{mn}, \\ V_{2,33}^{mn} &= c_2 V_1^{mn} + c_6 V_2^{mn} + c_7 V_3^{mn} + c_4 V_{2,3}^{mn} + c_8 V_{3,3}^{mn}, \\ V_{3,33}^{mn} &= c_9 V_1^{mn} + c_{10} V_2^{mn} + c_{11} V_3^{mn} + c_{12} V_{1,3}^{mn} + c_{13} V_{2,3}^{mn} + c_{14} V_{3,3}^{mn}, \end{aligned} \tag{3.5}$$

where the functions $c_i(x_3)$ $(i = \overline{1, 14})$ are displayed in Appendix B. For the sake of convenience we introduce the state variables

$$\begin{aligned} &S_1(x_3) = V_1^{mn}(x_3), \quad S_2(x_3) = V_2^{mn}(x_3), \quad S_3(x_3) = V_3^{mn}(x_3), \\ &S_4(x_3) = V_{1,3}^{mn} = S_{1,3}, \ S_5(x_3) = V_{2,3}^{mn} = S_{2,3}, \ S_6(x_3) = V_{3,3}^{mn} = S_{3,3}. \end{aligned} \tag{3.6}$$

Eq. (3.5) may be reduced to the matrix form

$$\{S_{,3}\} = [D]\{S\}, \tag{3.7}$$

where

$$\{S\} = \begin{Bmatrix} S_1 \\ S_2 \\ \vdots \\ S_6 \end{Bmatrix}, \tag{3.8}$$

$$[D] = \begin{bmatrix} 0 & 0 & 0 & 1 & 0 & 0 \\ 0 & 0 & 0 & 0 & 1 & 0 \\ 0 & 0 & 0 & 0 & 0 & 1 \\ c_1 & c_2 & c_3 & c_4 & 0 & c_5 \\ c_2 & c_6 & c_7 & 0 & c_4 & c_8 \\ c_9 & c_{10} & c_{11} & c_{12} & c_{13} & c_{14} \end{bmatrix}. \tag{3.9}$$

Using the definition for Lamé's coefficients given in Eq. (2.7) one obtains the formal solution to Eq. (3.7) as

$$\{S\} = [R] \begin{bmatrix} \mathrm{e}^{\xi_1 x_3} & & & 0 \\ & \mathrm{e}^{\xi_2 x_3} & & \\ & & \ddots & \\ 0 & & & \mathrm{e}^{\xi_6 x_3} \end{bmatrix} [R]^{-1} \{K\}, \tag{3.10}$$

where $K_1, K_2, \ldots, K_6$ are arbitrary unknown complex constants connected with the boundary conditions. Here $[R]$ is the matrix of eigenvector; $[R]^{-1}$ is the inverse of the matrix $[R]$; and ξ_i $(i = \overline{1,6})$ denotes the eigenvalues associated with the matrix $[D]$. The elements ξ_j are defined in Appendix C. Equations (3.10) can alternatively be presented as

$$S_i = \sum_{j=1}^{6} s_{ij} e^{\xi_j x_3} K_j, \quad i = 1, 2, \ldots, 6. \tag{3.11}$$

According to Eq. (3.6), one can easily obtain

$$V_i^{mn} = \sum_{j=1}^{6} v_{ij} e^{\xi_j x_3} K_j, \quad i = 1, 2, 3, \tag{3.12}$$

where the elements v_{ij} and ξ_j are defined in Appendix D. In addition, the stresses can be obtained in terms of the displacements and their derivatives with respect to x_3 as

$$\begin{aligned}
\sigma_{11} &= e^{k(x_3/h+1/2)} \sum_{m=1}^{\infty} \sum_{n=1}^{\infty} \left(-\alpha_m (2\mu_0 + \lambda_0) V_1^{mn} - \lambda_0 \beta_n V_2^{mn} + \lambda_0 V_{3,3}^{mn}\right) \\
&\quad \times \sin(\alpha_m x_1) \sin(\beta_n x_2), \\
\sigma_{22} &= e^{k(x_3/h+1/2)} \sum_{m=1}^{\infty} \sum_{n=1}^{\infty} \left(-\lambda_0 \alpha_m V_1^{mn} - \beta_n (2\mu_0 + \lambda_0) V_2^{mn} + \lambda_0 V_{3,3}^{mn}\right) \\
&\quad \times \sin(\alpha_m x_1) \sin(\beta_n x_2), \\
\sigma_{33} &= e^{k(x_3/h+1/2)} \sum_{m=1}^{\infty} \sum_{n=1}^{\infty} \left(-\lambda_0 \alpha_m V_1^{mn} - \lambda_0 \beta_n V_2^{mn} + (2\mu_0 + \lambda_0) V_{3,3}^{mn}\right) \\
&\quad \times \sin(\alpha_m x_1) \sin(\beta_n x_2), \\
\sigma_{23} &= e^{k(x_3/h+1/2)} \sum_{m=1}^{\infty} \sum_{n=1}^{\infty} \mu_0 \left(V_{2,3}^{mn} + \beta_n V_3^{mn}\right) \sin(\alpha_m x_1) \cos(\beta_n x_2), \\
\sigma_{13} &= e^{k(x_3/h+1/2)} \sum_{m=1}^{\infty} \sum_{n=1}^{\infty} \mu_0 \left(V_{1,3}^{mn} + \alpha_m V_3^{mn}\right) \cos(\alpha_m x_1) \sin(\beta_n x_2), \\
\sigma_{12} &= e^{k(x_3/h+1/2)} \sum_{m=1}^{\infty} \sum_{n=1}^{\infty} \mu_0 \left(\beta_n V_1^{mn} + \alpha_m V_2^{mn}\right) \cos(\alpha_m x_1) \cos(\beta_n x_2).
\end{aligned} \tag{3.13}$$

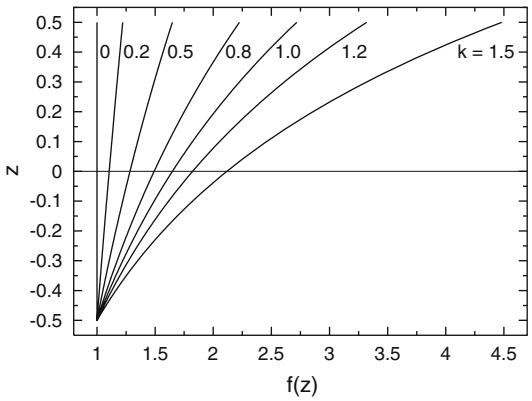

Fig. 2 The exponential variation function $f(z)$ along the thickness of an EG rectangular plate

To obtain the displacements and stresses of the EGM plate, we must satisfy the stress boundary conditions at the top and bottom surfaces of the plate. These conditions are

$$\begin{aligned}&\sigma_{13}\left(x_1, x_2, \mp\tfrac{h}{2}\right) = \sigma_{23}\left(x_1, x_2, \mp\tfrac{h}{2}\right) = \sigma_{33}\left(x_1, x_2, -\tfrac{h}{2}\right) = 0,\\ &\sigma_{33}\left(x_1, x_2, +\tfrac{h}{2}\right) = q(x_1, x_2).\end{aligned} \tag{3.14}$$

Equations (3.11) and (3.13), in conjunction with the above boundary conditions and with the aid of Eq. (2.15), determine the arbitrary constants $K_1, K_2, \ldots, K_6$.

4 Numerical results and discussion

Since 3-D elasticity solutions for homogeneous plates are available in the literature, we restrict our attention to inhomogeneous rectangular plates under sinusoidal loading. Based on the analysis of the foregoing sections, the stresses and displacements of simply supported EGM plates are obtained by the solution of trigonometric shear deformation plate theory (TPT) and elasticity theory. The state-space approach used in conjunction with the 3-D elasticity equations of EGM plates enables one to analyse the behaviour in bending of rectangular EGM plates. It is a tool of a great computational convenience and a compact vehicle for analytic manipulation.

Nondimensionalised displacements and stresses given here are presented according to the following definitions:

$$[u, v, w] = \frac{10E_0h^3}{a^4q_0}[v_1, v_2, v_3](z), \quad [\sigma_1, \sigma_2] = \frac{h^2}{a^2q_0}[\sigma_{11}, \sigma_{22}](z),$$
$$\sigma_6 = \frac{10h^2}{a^2q_0}\sigma_{12}(z), \quad [\sigma_4, \sigma_5] = \frac{h}{a\,q_0}[\sigma_{23}, \sigma_{13}](z), \quad z = \frac{x_3}{h}.$$

Numerical results are presented for various values of the aspect ratios (a/b) and the parameter k. Poisson's ratio is chosen as $\nu = 0.3$. Plots of the exponential function $f(z)$ along the thickness of an EGM plate are given in Fig. 2 for different values of the parameter k. The stresses σ_1 and σ_2 and transverse deflection w are computed at coordinates $x_1 = a/2, x_2 = b/2$; the transverse shear stress σ_5 and the in-plane displacement u are computed at $x_1 = a/2, x_2 = 0$; the transverse shear stress σ_4 and the in-plane displacement v are computed at $x_1 = 0, x_2 = b/2$; and the in-plane transverse stress σ_6 is computed at $x_1 = 0, x_2 = 0$.

Tables 1 and 2 contain the maximum deflection w of the mid-plane and the maximum value of the in-plane normal stress σ_2 for square and rectangular thick EGM plates. Two values of the side-to-thickness ratio, $a/h = 2$ and 4, and different values of the parameter k are used. The results of the 3-D elasticity solution are compared with the values obtained from the TPT. For the sake of completeness and comparison, results of higher-order shear deformation plate theory (HPT) are also included in these tables. The results for the deflection w decrease with the increase of both values of the parameter k and the aspect ratio a/b. The in-plane normal stress σ_2 increases as the parameter k increases, irrespective of the ratios a/b and a/h; σ_2 increases as the aspect ratio increases, approaching its largest value at $a/b = 1/2$, and then decreases again for a square

Table 1 Dimensionless deflection $w(0)$ for an EGM square plate

a/b	Theory	k					
		0.1	0.3	0.5	0.7	1.0	1.5
$a/h = 2$							
$\frac{1}{6}$	3-D	1.63774	1.48846	1.35184	1.22688	1.05929	0.82606
	TPT	1.62939	1.47309	1.33066	1.20101	1.02823	0.79056
	HPT	1.54777	1.39964	1.26493	1.14249	0.97956	0.75560
$\frac{1}{5}$	3-D	1.60646	1.46007	1.32607	1.20349	1.03907	0.81024
	TPT	1.59825	1.44493	1.30522	1.17804	1.00856	0.77540
	HPT	1.51991	1.37444	1.24214	1.12188	0.96184	0.74184
$\frac{1}{4}$	3-D	1.55146	1.41013	1.28074	1.16235	1.00352	0.78241
	TPT	1.54348	1.39541	1.26048	1.13764	0.97395	0.74874
	HPT	1.47089	1.33009	1.20201	1.08559	0.93065	0.71762
$\frac{1}{3}$	3-D	1.44295	1.31160	1.19129	1.08117	0.93337	0.72750
	TPT	1.43542	1.29771	1.17221	1.05795	0.90567	0.69615
	HPT	1.37394	1.24238	1.12269	1.01386	0.86898	0.66977
$\frac{1}{2}$	3-D	1.19445	1.08593	0.98640	0.89520	0.77266	0.60174
	TPT	1.18798	1.07399	0.97009	0.87548	0.74936	0.57578
	HPT	1.15080	1.04052	0.94012	0.84878	0.72712	0.55975
1	3-D	0.57693	0.52473	0.47664	0.43240	0.37269	0.28904
	TPT	0.57308	0.51806	0.46788	0.42216	0.36117	0.27712
	HPT	0.58586	0.52955	0.47814	0.43127	0.36871	0.28246
$a/h = 4$							
$\frac{1}{6}$	3-D	1.17140	1.06218	0.96331	0.87378	0.75501	0.59193
	TPT	1.16681	1.05509	0.95345	0.86107	0.73821	0.56969
	HPT	1.00649	0.91087	0.82448	0.74640	0.64306	0.50178
$\frac{1}{5}$	3-D	1.14589	1.03906	0.94236	0.85478	0.73859	0.57904
	TPT	1.14140	1.03210	0.93268	0.84231	0.72212	0.55726
	HPT	0.98508	0.89150	0.80694	0.73050	0.62935	0.49105
$\frac{1}{4}$	3-D	1.10115	0.99852	0.90560	0.82145	0.70979	0.55643
	TPT	1.09682	0.99180	0.89625	0.80941	0.69390	0.53546
	HPT	0.94753	0.85750	0.77615	0.70262	0.60529	0.47222
$\frac{1}{3}$	3-D	1.01338	0.91899	0.83350	0.75606	0.65329	0.51209
	TPT	1.00938	0.91272	0.82479	0.74486	0.63854	0.49270
	HPT	0.87379	0.79076	0.71571	0.64787	0.55806	0.43525
$\frac{1}{2}$	3-D	0.81529	0.73946	0.67075	0.60846	0.52574	0.41200
	TPT	0.81202	0.73425	0.66350	0.59917	0.51361	0.39620
	HPT	0.70700	0.63979	0.57901	0.52405	0.45126	0.35169
1	3-D	0.34900	0.31677	0.28747	0.26083	0.22534	0.18054
	TPT	0.34749	0.31419	0.28388	0.25631	0.21961	0.16922
	HPT	0.31111	0.28146	0.25461	0.23027	0.19800	0.15377

plate. In general, it is clear that the present TPT gives more accurate results than HPT when compared to the 3-D elasticity solutions.

Variations of the displacements and stresses through the thickness of EGM plates are shown graphically in Figs. 3–16. The results for $a/h = 4$ are presented here. It is assumed (unless otherwise stated) that $k = 0.5$ and $a/b = 1/3$. Figures 3–9 show the plots of displacements u, v and w and of the stresses σ_1, σ_6, σ_5 and σ_4 for different values of the aspect ratio a/b. Similar results for different values of the parameter k are given in Figs. 10–16.

The displacements and stresses do not vary as linear functions of the thickness coordinate z because the plate is EG and the material properties are functions of z. The displacements u and v and stresses σ_1 and σ_6 predicted by the TPT are in excellent agreement with the exact 3-D solution (see Figs. 3, 4, 6, 7, 10, 11, 13, and 14). The tensile and compressive values of the longitudinal stress, σ_1 (cf. Figs. 6 and 13), come to a maximum at a point on the top and bottom surfaces of the EGM plate, respectively. The maximum tensile and compressive values increase as the aspect ratio decreases as shown in Fig. 6. While Fig. 13 shows that the maximum tensile value of σ_1 occurs at the top surface for the largest value of the parameter k, the maximum compressive value occurs at the bottom surface for the smallest value of k.

Figure 5 shows that the TPT underestimates the transverse deflection w at points above the middle plate. For large values of k the TPT underestimates the transverse deflection at all points within the plate (see Fig. 12).

Table 2 Dimensionless stress $\sigma_2(1/2)$ for an EGM square plate

a/b	Theory	k					
		0.1	0.3	0.5	0.7	1.0	1.5
$a/h = 2$							
$\frac{1}{6}$	3-D	0.29429	0.31008	0.32699	0.34508	0.37456	0.43051
	TPT	0.29119	0.31184	0.33385	0.35731	0.39547	0.46786
	HPT	0.31192	0.33462	0.35873	0.38433	0.42573	0.50345
$\frac{1}{5}$	3-D	0.29674	0.31277	0.32993	0.34829	0.37821	0.43500
	TPT	0.29353	0.31439	0.33662	0.36032	0.39884	0.47187
	HPT	0.31327	0.33607	0.36030	0.38604	0.42764	0.50573
$\frac{1}{4}$	3-D	0.30084	0.31727	0.33486	0.35368	0.38435	0.44257
	TPT	0.29743	0.31864	0.34124	0.36533	0.40446	0.47857
	HPT	0.31543	0.33842	0.36285	0.38878	0.43072	0.50943
$\frac{1}{3}$	3-D	0.30808	0.32525	0.34362	0.36329	0.39534	0.45619
	TPT	0.30421	0.32606	0.34933	0.37410	0.41432	0.49035
	HPT	0.31890	0.34220	0.36695	0.39323	0.43572	0.51545
$\frac{1}{2}$	3-D	0.31998	0.33849	0.35833	0.37956	0.41417	0.47989
	TPT	0.31463	0.33758	0.36200	0.38796	0.43003	0.50925
	HPT	0.32223	0.34592	0.37109	0.39782	0.44102	0.52203
1	3-D	0.31032	0.32923	0.34953	0.37127	0.40675	0.47405
	TPT	0.29554	0.31811	0.34208	0.36750	0.40851	0.48508
	HPT	0.28882	0.31072	0.33398	0.35866	0.39852	0.47305
$a/h = 4$							
$\frac{1}{6}$	3-D	0.21814	0.23211	0.24699	0.26284	0.28857	0.33725
	TPT	0.23686	0.25204	0.26830	0.28574	0.31441	0.36990
	HPT	0.28170	0.30133	0.32219	0.34435	0.38024	0.44786
$\frac{1}{5}$	3-D	0.22060	0.23476	0.24984	0.26591	0.29199	0.34133
	TPT	0.23912	0.25450	0.27097	0.28863	0.31764	0.37371
	HPT	0.28261	0.30231	0.32323	0.34547	0.38148	0.44934
$\frac{1}{4}$	3-D	0.22470	0.23918	0.25460	0.27103	0.29770	0.34816
	TPT	0.24286	0.25858	0.27539	0.29342	0.32299	0.38004
	HPT	0.28399	0.30379	0.32483	0.34719	0.38338	0.45159
$\frac{1}{3}$	3-D	0.23188	0.24692	0.26295	0.28002	0.30775	0.36021
	TPT	0.24931	0.26563	0.28307	0.30174	0.33230	0.39106
	HPT	0.28588	0.30583	0.32702	0.34954	0.38601	0.45471
$\frac{1}{2}$	3-D	0.24314	0.25913	0.27618	0.29434	0.32385	0.37968
	TPT	0.25878	0.27609	0.29456	0.31428	0.34644	0.40788
	HPT	0.28539	0.30534	0.32655	0.34908	0.38556	0.45428
1	3-D	0.22472	0.23995	0.25621	0.27356	0.30177	0.35885
	TPT	0.23457	0.25098	0.26842	0.28698	0.31706	0.37386
	HPT	0.24080	0.25783	0.27593	0.29515	0.32627	0.38482

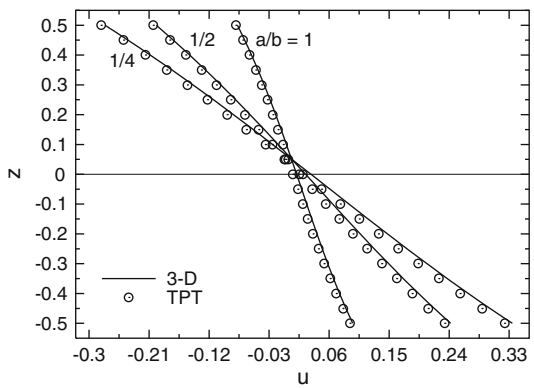

Fig. 3 The variation of u through the thickness of an EG rectangular plate ($k = 0.5, a/h = 4$)

As seen from Figs. 8, 9, 15, and 16, the maximum values of the out-of-plane transverse shear stresses σ_5 and σ_4 do not occur at $z = 0$. These maximum values occur at points a little above the mid-plane of the EGM plate. There is an error exhibited by TPT for σ_5 and σ_4 through the thickness of the plate. The largest

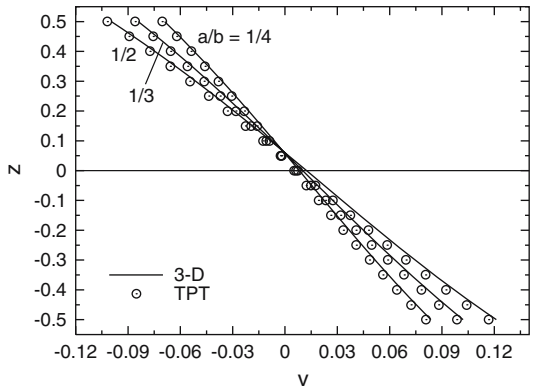

Fig. 4 The variation of v through the thickness of an EG rectangular plate ($k = 0.5, a/h = 4$)

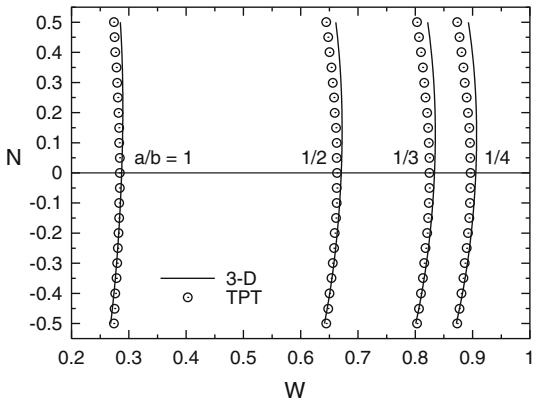

Fig. 5 The variation of w through the thickness of an EG rectangular plate ($k = 0.5, a/h = 4$)

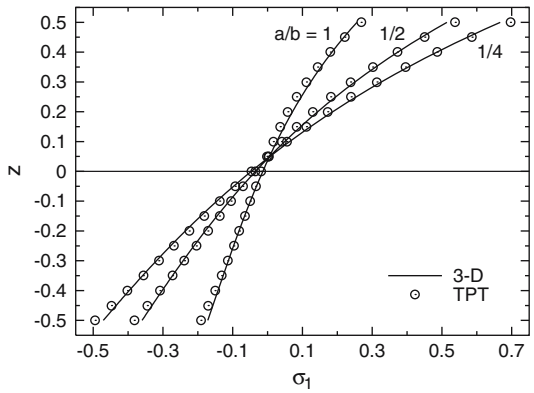

Fig. 6 The variation of σ_1 through the thickness of an EG rectangular plate ($k = 0.5, a/h = 4$)

errors occur at points in which the transverse shear stresses reach their maximum values. Errors increase as k increases (see Figs. 15 and 16) and as a/b decreases for σ_5 (see Fig. 8) and increases for σ_4 (see Fig. 9).

Note that the through-the-thickness distributions of stresses and displacements strongly depend on the aspect ratio of the plate. In addition, results are affected strongly by the exponentially graded parameter k. In general, the prediction of the displacements and stresses resulting from TPT yields results rather close to those obtained by the 3-D elasticity solution.

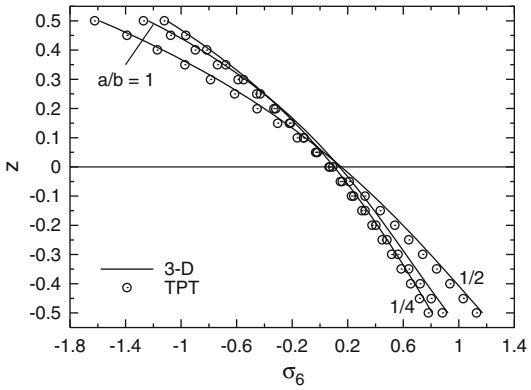

Fig. 7 The variation of σ_6 through the thickness of an EG rectangular plate ($k = 0.5, a/h = 4$)

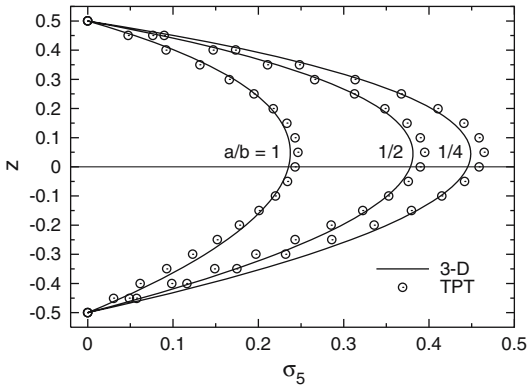

Fig. 8 The variation of σ_5 through the thickness of an EG rectangular plate ($k = 0.5, a/h = 4$)

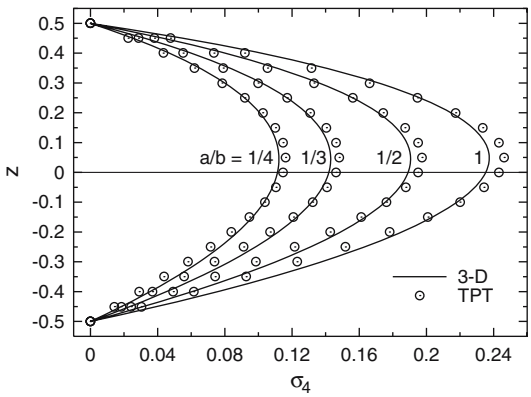

Fig. 9 The variation of σ_4 through the thickness of an EG rectangular plate ($k = 0.5, a/h = 4$)

5 Concluding remarks

We have considered the bending analysis of a simply supported exponentially graded rectangular plate subjected to a sinusoidal pressure. The effective material properties at points in the plate are assumed to vary in the thickness direction only according to a simple exponential law. When we presume trigonometric variations of the displacements that identically satisfy boundary conditions at the edges, we derive ordinary differential equations for the through-the-thickness variation of functions and solve them analytically. A more general procedure for solving the exact 3-D elasticity equations is developed, and extensive numerical results are generated. The exact 3-D solution of the problem studied here is compared with those obtained by the trigonometric and higher-order plate theories. For thick exponentially graded plates, the present trigonometric theory

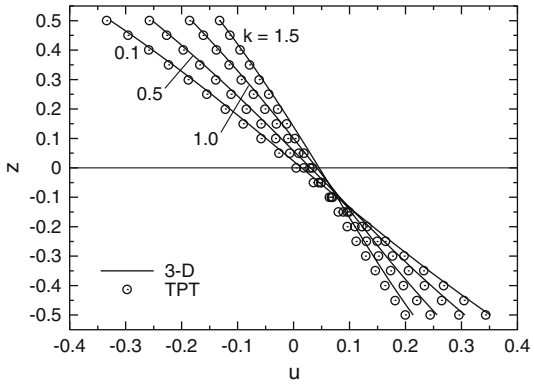

Fig. 10 The variation of u through the thickness of an EG rectangular plate ($b = 3a, a/h = 4$)

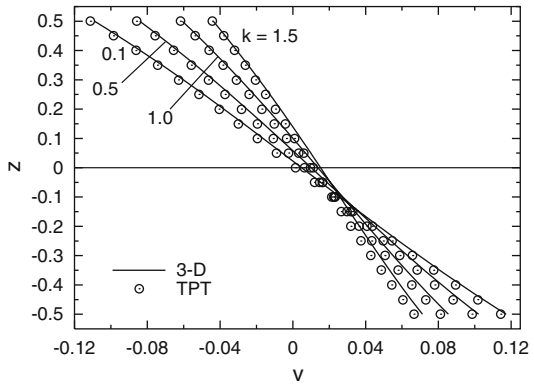

Fig. 11 The variation of v through the thickness of an EG rectangular plate ($b = 3a, a/h = 4$)

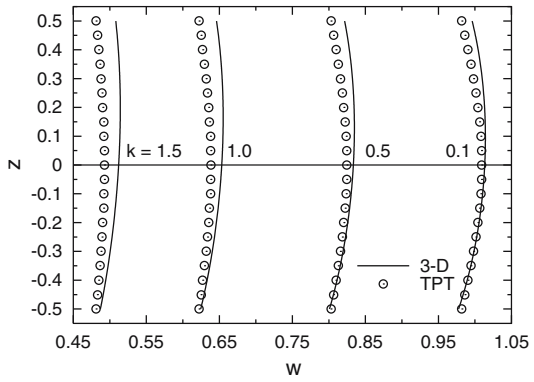

Fig. 12 The variation of w through the thickness of an EG rectangular plate ($b = 3a, a/h = 4$)

predicts displacements and stresses more accuracy when compared to the higher-order shear deformation plate theory. In general, the exact and trigonometric solutions presented here provide benchmark results, which can be used for the evaluation of different plate theories and also to compare results obtained by other approximate methods such as the finite-element method.

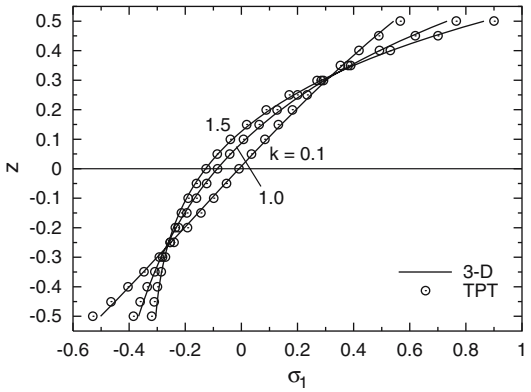

Fig. 13 The variation of σ_1 through the thickness of an EG rectangular plate ($b = 3a, a/h = 4$)

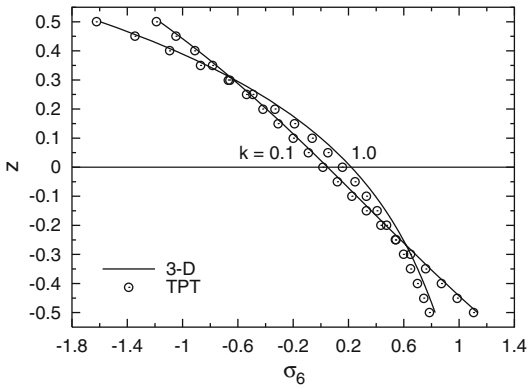

Fig. 14 The variation of σ_6 through the thickness of an EG rectangular plate ($b = 3a, a/h = 4$)

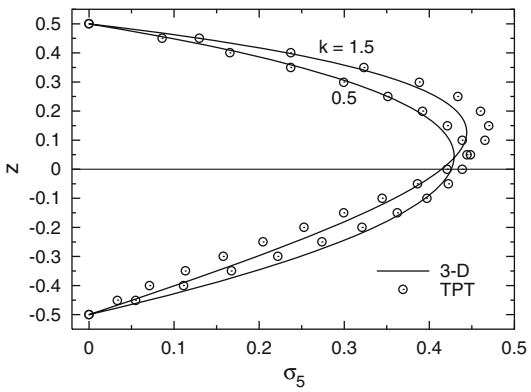

Fig. 15 The variation of σ_5 through the thickness of an EG rectangular plate ($b = 3a, a/h = 4$)

Appendix A

The elements $L_{ij} = L_{ji}$ of the coefficient matrix $[L]$, which appeared in Eq. (2.19), are given by

$$
\begin{aligned}
L_{11} &= -\alpha_m^2 \left(A^{11} + B^{11}\right) - \tfrac{1}{2}\beta_n^2 A^{11}, \\
L_{12} &= -\alpha_m \beta_n \left(\tfrac{1}{2}A^{11} + B^{11}\right), \\
L_{13} &= \alpha_m \left(\alpha_m^2 + \beta_n^2\right)\left(A^{12} + B^{12}\right), \\
L_{14} &= -\alpha_m^2 \left(A^{13} + B^{13}\right) - \tfrac{1}{2}\beta_n^2 A^{13},
\end{aligned}
$$

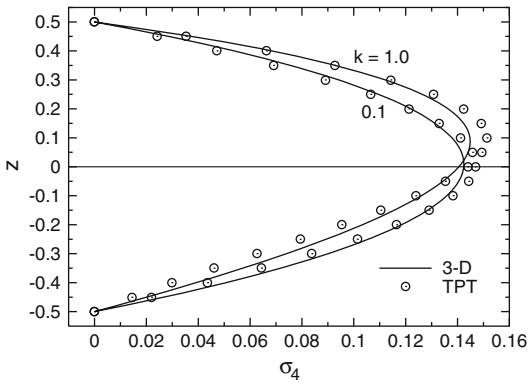

Fig. 16 The variation of σ_4 through the thickness of an EG rectangular plate ($b = 3a, a/h = 4$)

$$
\begin{aligned}
L_{15} &= -\alpha_m\beta_n\left(\tfrac{1}{2}A^{13} + B^{13}\right),\\
L_{16} &= \alpha_m C^{11},\\
L_{22} &= -\beta_n^2\left(A^{11} + B^{11}\right) - \tfrac{1}{2}\alpha_m^2 A^{11},\\
L_{23} &= \beta_n\left(\alpha_m^2 + \beta_n^2\right)\left(A^{12} + B^{12}\right),\\
L_{24} &= L_{15},\\
L_{25} &= -\beta_n^2\left(A^{13} + B^{13}\right) - \tfrac{1}{2}\alpha_m^2 A^{13},\\
L_{26} &= \beta_n C^{11},\\
L_{33} &= -\left(\alpha_m^2 + \beta_n^2\right)^2\left(A^{22} + B^{22}\right),\\
L_{34} &= \alpha_m\left(\alpha_m^2 + \beta_n^2\right)\left(A^{23} + B^{23}\right),\\
L_{35} &= \beta_n\left(\alpha_m^2 + \beta_n^2\right)\left(A^{23} + B^{23}\right),\\
L_{36} &= -\left(\alpha_m^2 + \beta_n^2\right)C^{12},\\
L_{44} &= -\alpha_m^2\left(A^{33} + B^{33}\right) - \tfrac{1}{2}\beta_n^2 A^{33} - c^*,\\
L_{45} &= -\alpha_m\beta_n\left(\tfrac{1}{2}A^{33} + B^{33}\right),\\
L_{46} &= \alpha_m\left(C^{13} - c^*\right),\\
L_{55} &= -\beta_n^2\left(A^{33} + B^{33}\right) - \tfrac{1}{2}\alpha_m^2 A^{33} - c^*,\\
L_{56} &= \beta_n\left(C^{13} - c^*\right),\\
L_{66} &= -\left(\alpha_m^2 + \beta_n^2\right)c^* - c.
\end{aligned}
$$

Appendix B

The elements $c_i(x_3)$ $(i = \overline{1, 14})$ defined in Eqs. (3.5) are given by

$$
\begin{aligned}
&c_1 = \alpha_m^2\left(2 + \tfrac{\lambda}{\mu}\right) + \beta_n^2, && c_2 = \alpha_m\beta_n\left(1 + \tfrac{\lambda}{\mu}\right),\\
&c_3 = -\tfrac{\alpha_m\mu_{,3}}{\mu}, && c_4 = -\tfrac{\mu_{,3}}{\mu},\\
&c_5 = -\alpha_m\left(1 + \tfrac{\lambda}{\mu}\right), && c_6 = \alpha_m^2 + \beta_n^2\left(2 + \tfrac{\lambda}{\mu}\right),\\
&c_7 = -\tfrac{\beta_n\mu_{,3}}{\mu}, && c_8 = -\beta_n\left(1 + \tfrac{\lambda}{\mu}\right),\\
&c_9 = \tfrac{\alpha_m\lambda_{,3}}{2\mu+\lambda}, && c_{10} = \tfrac{\beta_n\lambda_{,3}}{2\mu+\lambda},\\
&c_{11} = \tfrac{\mu\left(\alpha_m^2+\beta_n^2\right)}{2\mu+\lambda}, && c_{12} = \tfrac{\alpha_m(\mu+\lambda)}{2\mu+\lambda},\\
&c_{13} = \tfrac{\beta_n(\mu+\lambda)}{2\mu+\lambda}, && c_{14} = -\tfrac{(2\mu+\lambda)_{,3}}{2\mu+\lambda}.
\end{aligned}
$$

Appendix C

The elements ξ_j, which appeared in Eq. (3.10), are given by

$$\begin{aligned}
&\xi_1 = \tfrac{1}{2}(a_1 - \bar{k}), \qquad \xi_2 = -\tfrac{1}{2}(a_1 + \bar{k}),\\
&\xi_3 = -\tfrac{a_2+\bar{k}(2\bar{\mu}_0+1)}{2(2\bar{\mu}_0+1)},\ \xi_4 = \tfrac{a_2-\bar{k}(2\bar{\mu}_0+1)}{2(2\bar{\mu}_0+1)},\\
&\xi_5 = -\tfrac{a_3+\bar{k}(2\bar{\mu}_0+1)}{2(2\bar{\mu}_0+1)},\ \xi_6 = \tfrac{a_3-\bar{k}(2\bar{\mu}_0+1)}{2(2\bar{\mu}_0+1)},
\end{aligned}$$

where

$$\begin{aligned}
a_1^2 &= 4\left(\alpha_m^2 + \beta_n^2\right) + \bar{k}^2,\\
a_2^2 &= (2\bar{\mu}_0 + 1)\left[a_1^2(2\bar{\mu}_0 + 1) - 4a_0\right],\\
a_3^2 &= (2\bar{\mu}_0 + 1)\left[a_1^2(2\bar{\mu}_0 + 1) + 4a_0\right],
\end{aligned}$$

in which

$$a_0^2 = -\bar{k}^2\,(2\bar{\mu}_0 + 1)\left(\alpha_m^2 + \beta_n^2\right), \quad \bar{k} = k/h, \ \ \bar{\mu}_0 = \mu_0/\lambda_0.$$

Appendix D

The elements v_{ij}, which appeared in Eq. (3.12), are given by

$$\begin{aligned}
&v_{11} = v_{12} = v_{13} = v_{14} = v_{15} = v_{16} = 1,\\
&v_{21} = v_{22} = -\tfrac{\alpha_m}{\beta_n}, \quad v_{23} = v_{24} = v_{25} = v_{26} = \tfrac{\beta_n}{\alpha_m},\\
&v_{31} = v_{32} = 0, \quad v_{3j} = \tfrac{1}{\Delta}\sum_{l=0}^{5} f_{jl}\bar{\mu}_0^l, \ \ j = 3, 4, 5, 6,
\end{aligned}$$

where

$$\Delta = 32\bar{k}^2\alpha_m(2\bar{\mu}_0 + 1)^3\left[b_0^2(2\bar{\mu}_0 + 1) + \bar{\mu}_0^2(\alpha_m^2 + \beta_n^2)\right],$$

in which

$$b_0^2 = \bar{k}^2 + \alpha_m^2 + \beta_n^2,$$

and the elements f_{jl} are given by

$$\begin{aligned}
f_{30} &= -4\bar{k}^5 + \left(4a_0 + a_1^2\right)\left(4\bar{k}^3 - a_2^3\right) - 4a_2\left(a_1^2 - a_2^2\right)\bar{k}^2 + a_1^4 a_2,\\
f_{31} &= -24\bar{k}^5 + 8\left(10a_0 + 3a_1^2\right)\bar{k}^3 - 4a_2\left(7a_1^2 - 3a_2^2\right)\bar{k}^2 + 8a_1^4 a_2 - 4a_2^3\left(2a_0 + a_1^2\right),\\
f_{32} &= -44\bar{k}^5 + 4\left(24a_0 + 11a_1^2\right)\bar{k}^3 - 8a_2\left(9a_1^2 - a_2^2\right)\bar{k}^2 + 25a_1^4 a_2 - a_2^3\left(4a_0 + 5a_1^2\right),
\end{aligned}$$

$$
\begin{aligned}
f_{33} &= -8\bar{k}^5 - 8\left(8a_0 - a_1^2\right)\bar{k}^3 - 80a_1^2a_2\bar{k}^2 + 38a_1^4a_2 - 2a_1^2a_2^3,\\
f_{34} &= 48\bar{k}^5 - 16\left(8a_0 + 3a_1^2\right)\bar{k}^3 - 32a_1^2a_2\bar{k}^2 + 28a_1^4a_2,\\
f_{35} &= 32\bar{k}^5 - 32a_1^2\bar{k}^3 + 8a_1^4a_2,\\
f_{40} &= -4\bar{k}^5 + 4\left(4a_0 + a_1^2\right)\bar{k}^3 + 4a_2\left(a_1^2 - a_2^2\right)\bar{k}^2 + a_2^3\left(4a_0 + a_1^2\right) - a_1^4a_2,\\
f_{41} &= -24\bar{k}^5 + 8\left(10a_0 + 3a_1^2\right)\bar{k}^3 + 4a_2\left(7a_1^2 - 3a_2^2\right)\bar{k}^2 - 8a_1^4a_2 + 4a_2^3\left(2a_0 + a_1^2\right),\\
f_{42} &= -44\bar{k}^5 + 4\left(24a_0 + 11a_1^2\right)\bar{k}^3 + 8a_2\left(9a_1^2 - a_2^2\right)\bar{k}^2 - 25a_1^4a_2 + a_2^3\left(4a_0 + 5a_1^2\right),\\
f_{43} &= -8\bar{k}^5 - 8\left(8a_0 - a_1^2\right)\bar{k}^3 + 80a_1^2a_2\bar{k}^2 - 38a_1^4a_2 + 2a_1^2a_2^3,\\
f_{44} &= 48\bar{k}^5 - 16\left(8a_0 + 3a_1^2\right)\bar{k}^3 + 32a_1^2a_2\bar{k}^2 - 28a_1^4a_2,\\
f_{45} &= 32\bar{k}^5 - 32a_1^2\bar{k}^3 - 8a_1^4a_2,\\
f_{50} &= -4\bar{k}^5 - \left(4a_0 - a_1^2\right)\left(4\bar{k}^3 - a_3^3\right) - 4a_3\left(a_1^2 - a_3^2\right)\bar{k}^2 + a_1^4a_3,\\
f_{51} &= -24\bar{k}^5 - 8\left(10a_0 - 3a_1^2\right)\bar{k}^3 - 4a_3\left(7a_1^2 - 3a_3^2\right)\bar{k}^2 + 8a_1^4a_3 + 4a_3^3\left(2a_0 - a_1^2\right),\\
f_{52} &= -44\bar{k}^5 - 4\left(24a_0 - 11a_1^2\right)\bar{k}^3 - 8a_3\left(9a_1^2 - a_3^2\right)\bar{k}^2 + 25a_1^4a_3 + a_3^3\left(4a_0 - 5a_1^2\right),\\
f_{53} &= -8\bar{k}^5 + 8\left(8a_0 + a_1^2\right)\bar{k}^3 - 80a_1^2a_3\bar{k}^2 + 38a_1^4a_3 - 2a_1^2a_3^3,\\
f_{54} &= 48\bar{k}^5 + 16\left(8a_0 - 3a_1^2\right)\bar{k}^3 - 32a_1^2a_3\bar{k}^2 + 28a_1^4a_3,\\
f_{55} &= 32\bar{k}^5 - 32a_1^2\bar{k}^3 + 8a_1^4a_3,\\
f_{60} &= -4\bar{k}^5 - 4\left(4a_0 - a_1^2\right)\bar{k}^3 + 4a_3\left(a_1^2 - a_3^2\right)\bar{k}^2 - a_3^3\left(4a_0 - a_1^2\right) - a_1^4a_3,\\
f_{61} &= -24\bar{k}^5 - 8\left(10a_0 - 3a_1^2\right)\bar{k}^3 + 4a_3\left(7a_1^2 - 3a_3^2\right)\bar{k}^2 - 8a_1^4a_3 - 4a_3^3\left(2a_0 - a_1^2\right),\\
f_{62} &= -44\bar{k}^5 - 4\left(24a_0 - 11a_1^2\right)\bar{k}^3 + 8a_3\left(9a_1^2 - a_3^2\right)\bar{k}^2 - 25a_1^4a_3 - a_3^3\left(4a_0 - 5a_1^2\right),\\
f_{63} &= -8\bar{k}^5 + 8\left(8a_0 + a_1^2\right)\bar{k}^3 + 80a_1^2a_3\bar{k}^2 - 38a_1^4a_3 + 2a_1^2a_3^3,\\
f_{64} &= 48\bar{k}^5 + 16\left(8a_0 - 3a_1^2\right)\bar{k}^3 + 32a_1^2a_3\bar{k}^2 - 28a_1^4a_3,\\
f_{65} &= 32\bar{k}^5 - 32a_1^2\bar{k}^3 - 8a_1^4a_3.
\end{aligned}
$$

References

1. Yamanouchi, M., Koizumi, M., Hirai, T., Shiota, I.: Proceeding of the First International Symposium on Functionally Gradient Materials. Sendai, Japan (1990)
2. Koizumi, M.: The concept of FGM. Ceram. Trans. Funct. Gradient Mater. **34**, 3–10 (1993)
3. Praveen, G.N., Reddy, J.N.: Nonlinear transient thermoelastic analysis of functionally graded ceramic-metal plates. Int. J. Solids Struct. **35**, 4457–4476 (1998)
4. Reddy J.N., Chin, C.D.: Thermomechanical analysis of functionally graded cylinders and plates. J. Ther. Stresses **21**, 593–626 (1998)
5. Loy, C.T., Lam, K.Y., Reddy, J.N.: Vibration of functionally graded cylindrical shells. Int. J. Mech. Sci. **41**, 309–324 (1999)
6. Reddy, J.N.: Analysis of functionally graded plates. Int. J. Numer. Methods Eng. **47**, 663–684 (2000)
7. Cheng, Z.Q., Batra, R.C.: Deflection relationships between the homogeneous Kirchhoff plate theory and different functionally graded plate theories. Arch. Mech. **52**, 143–158 (2000)
8. Cheng, Z.Q., Batra, R.C.: Exact correspondence between eigenvalues of membranes and functionally graded simply supported polygonal plates. J. Sound Vib. **229**, 879–895 (2000)
9. Cheng, Z.Q., Batra, R.C.: Three-dimensional thermoelastic deformations of a functionally graded elliptic plate. Composites B **31**, 97–106 (2000)
10. Vel, S.S., Batra, R.C.: Exact solution for thermoelastic deformations of functionally graded thick rectangular plates. AIAA J. **40**, 1421–1433 (2002)
11. Whitney, J.M., Pagano, N.J.: Shear deformation in heterogeneous anisotropic plates. ASME J. Appl. Mech. **37**, 1031–1036 (1970)
12. Bert, C. W.: Simplified analysis of elastic shear factors for beams of nonhomogeneous cross-section. J. Compos. Mater. **7**, 525–529 (1973)
13. Librescu, L.: Elastostatics and kinetics of anisotropic and heterogeneous shell-type structures. Noordhoff, Leiden, The Netherlands (1975)
14. Reissner, E.: A mixed variational equation for a twelfth-order theory of bending of nonhomogeneous transversely isotropic plates. Comput. Mech. **7**, 355–360 (1991)

15. Reissner, E.: On the equations of an eighth-order theory of nonhomogeneous transversely isotropic plates. Int. J. Solids Struct. **31**, 89–96 (1994)
16. Fares, M.E., Zenkour, A.M.: Buckling and free vibration of non-homogeneous composite cross-ply laminated plates with various plate theories. Compos. Struct. **44**, 279–287 (1999)
17. Zenkour, A.M., Fares, M.E.: Non-homogeneous response of cross-ply laminated elastic plates using a higher-order theory. Compos. Struct. **44**, 297–305 (1999)
18. Zenkour, A.M., Fares, M.E.: Bending, buckling and free vibration of non-homogeneous cross-ply laminated cylindrical shells using a refined first-order theory. Composites B **32**, 237–247 (2001)
19. Lo, K.H., Christensen, R.M., Wu, E.M.: A higher-order theory of plate deformation, Part 1: homogeneous plates. ASME J. Appl. Mech. **44**, 669–676 (1977)
20. Reddy, J.N.: A simple higher-order theory for laminated composite plates. ASME J. Appl. Mech. **51**, 745–752 (1984)
21. Reddy, J.N.: A generalization of two-dimensional theories of laminated composite plates. Commun. Appl. Numer. Meth. **3**, 173–180 (1987)
22. Noor, A.K., Burton, W.S.: Assessment of shear deformation theories for multilayered composite plates. Appl. Mech. Rev. **42**, 1–12 (1989)
23. Reddy, J.N.: A general third-order nonlinear theory of plates with moderate thickness. Int. J. Nonlin, Mech. **25**, 677–686 (1990)
24. Reddy, J.N.: A review of refined theories of laminated composite plates. Shock Vib. Digest **22**, 3–17 (1990)
25. Zenkour, A.M.: Analytical solution for bending of cross-ply laminated plates under thermo-mechanical loading. Compos. Struct. **65**, 367–379 (2004)
26. Zenkour, A.M.: Buckling of fiber-reinforced viscoelastic composite plates using various plate theories. J. Eng. Math. **50**, 75–93 (2004)
27. Zenkour, A.M.: Thermal effects on the bending response of fiber-reinforced viscoelastic composite plates using a sinusoidal shear deformation theory. Acta. Mech. **171**, 171–187 (2004)
28. Zenkour, A.M.: A comprehensive analysis of functionally graded sandwich plates: Part 1—Deflection and stresses, Part 2—Buckling and free vibration. Int. J. Solids Struct. **42**, 5224–5258 (2005)
29. Zenkour, A.M.: On vibration of functionally graded plates according to a refined trigonometric plate theory. Int. J. Struct. Stab. Dynam. **5**, 279–297 (2005)
30. Zenkour, A.M.: Generalized shear deformation theory for bending analysis of functionally graded plates. Appl. Math. Model. **30**, 67–84 (2006)
31. Zenkour, A.M.: Three-dimensional elasticity solutions for uniformly loaded cross-ply laminates and sandwich plates. J. Sand. Struct. Mater. (in press)